5-2013

ZnO nanorods as catalyst for biodiesel production from olive oil.

Carmen Maria Miralda Molina 1990-
University of Louisville

ZNO NANORODS AS CATALYTS FOR BIODIESEL PRODUCTION FROM OLIVE OIL

By

Carmen Maria Miralda Molina
B.S. Ch.E., University of Louisville, May 2012

A Thesis
Submitted to the Faculty of the
University of Louisville
J. B. Speed School of Engineering
as Partial Fulfillment of the Requirements
for the Professional Degree

MASTER OF ENGINEERING

Department of Chemical Engineering

May 2013

ZNO NANORODS AS CATALYTS FOR BIODIESEL PRODUCTION FROM OLIVE OIL

Submitted by: _____
Carmen Maria Miralda Molina

A Thesis Approved On

_____
(Date)

by the Following Reading and Examination Committee:

_____
Dr. Moises Carreon, Thesis Director

_____
Dr. Gamini Sumanasekera

_____
Dr. Gerold Willing

ACKNOWLEDGEMENTS

It is difficult to describe the debt of gratitude I owe my family, specifically my parents. With their love, tenacity, and willingness to sacrifice themselves for my wellbeing they have made me the person I am today. The success I am achieving with the completion of my higher education is a product of their parenting. I hope I can give my children as much love and opportunities as my parents have given me.

I would also like to thank Dr. Moises A. Carreon, Dr. Gerold A. Willing, and Dr. James C. Watters for their teachings, mentorship, and friendship. In my time at the University of Louisville they have always guided me in the direction that would help me grow professionally and personally. Because of their dedication to their work, I feel well equipped to enter the professional world.

As part of what has become my "Chemical Engineering Family" I would also like to recognize William C. Hunter III, Patrick Kroeger, Logan Waller, and Patrick Baker. Throughout our coursework they have served as my support system. Completing even the most challenging assignments was always easier because of their company and academic brilliance.

Additionally I would like to thank Hugo Apolo Nambo Salgado for his assistance in the lab. Without his knowledge, expertise, and generosity the completion of this thesis work would not have been possible. It has been a pleasure to work and develop a friendship with him. Furthermore, I would like to thank Dr. Gamini Sumanasekera for sitting on my thesis defense committee.

ABSTRACT

The motivation to determine a viable alternative to petroleum based energy has risen in recent years due to increased greenhouse gas emissions, environmental pollution, and the fear of exhausting oil and natural gas reserves. Biodiesel derived from the transesterification of vegetable oils or animal fats has emerged as a viable alternative to petroleum diesel. However, for this to become an option available to the average consumer it is vital to find an effective catalyst. Metal oxides have emerged as potential heterogeneous catalysts. ZnO in particular is attractive because it is abundant. The use of nanostructures has been shown to improve the catalytic performance of ZnO.

ZnO nanorods were synthesized using a solution approach. The crystalline structure, morphology, and surface area were confirmed using XRD, SEM, and BET surface area respectively. The characterized nanorods were used as catalysts for the production of biodiesel. The nanorods achieved conversions of 94.8% at 150ºC for reaction times of eight hours. They also demonstrated better catalytic performance, attributed to their increased degree of crystallinity, than conventional ZnO.

A kinetic study at 150ºC to determine the reaction rate parameters was also conducted. Due to the presence of three distinct phases in the reaction, initially the reaction rate is dominated by mass transfer limitations. However, these are eventually overcome and the reaction proceeds with a pseudo-first order with respect to the oil and a reaction rate constant of 0.5136 h^{-1}.

TABLE OF CONTENTS

APPROVAL PAGE ..... **ii**
ACKNOWLEDGEMENTS ..... **iv**
ABSTRACT ..... **v**
TABLE OF CONTENTS ..... **vi**
NOMENCLATURE ..... **vii**
LIST OF TABLES ..... **ix**
LIST OF FIGURES ..... **x**

I. INTRODUCTION **1**

A. Biodiesel As A Viable Alternative To Petroleum-Based Diesel 1
B. Production Of Biodiesel 2
C. Homogeneous Vs. Heterogeneous Catalysis 5
D. Metal Oxides As Heterogeneous Base Catalysts 8
E. ZnO Nanostructures As Effective Catalysts For Biodiesel Production 10
F. ZnO Nanostructure Synthesis And Their Catalytic Potential 11
G. Theory Of Reaction Kinetics Modeling For ZnO Catalyzed Biodiesel Synthesis 13
H. Justification 17
I. Objectives 17

II. EXPERIMENTAL **18**

A. Synthesis of ZnO Nanorods 18
B. Characterization of ZnO Nanorods 18
C. Biodiesel Synthesis and Characterization 21

III. RESULTS AND DISCUSSION **26**

A. ZnO Nanorod Solution Synthesis and Characterization 26
B. ZnO Nanorods as Catalysts for Biodiesel Production 30
C. Reaction Kinetics of the ZnO Nanorod Catalyzed Biodiesel Reaction 35

IV. CONCLUSIONS **39**

VI. RECOMMENDATIONS **41**

A. ZnO Nanorod Synthesis and Catalytic Potential for Biodiesel Production 41
B. ZnO Nanorod Characterization 41
C. ZnO Nanorods Catalyzed Biodiesel Synthesis Kinetics 42

VII. REFERENCES **43**

VIII. APPENDIX: SUPPORTING INFORMATION **45**

A. Alternative ZnO Nanorod Synthesis Methods 45
B. Materials Characterization for Conventional ZnO 47
C. Kinetics of Reaction 48

VITA **51**

NOMENCLATURE

α	=	Order of Reaction with Respect to Triglycerides
β	=	Order of Reaction with Respect to Methanol
θ	=	Diffraction Angle (Degree)
µm	=	Micrometer
µmol	=	Micromole
^{1}H NMR	=	Proton Nuclear Magnetic Resonance
a.u.	=	Arbitrary Unit
$A_{\text{Methoxy Proton}}$	=	Area of Methoxy Proton Signal
$A_{\alpha\text{-Carbon Proton}}$	=	Area of α-Carbon Proton Signal
BET	=	Brunauer Emmett Teller
CaO	=	Calcium Oxide
cm^3	=	Cubic Centimeter
C_{MeOH}	=	Concentration of Methanol
CO	=	Carbon Monoxide
CO_2	=	Carbon Dioxide
C_{TG}	=	Concentration of Triglycerides
$C_{TG,0}$	=	Initial Concentration of Triglycerides
EDA	=	Ethylenediamiane
FAME	=	Fatty Acid Methyl Ester
FFA	=	Free Fatty Acid
FFA	=	Free Fatty Acid
G	=	Glycerol
g	=	Gram
h	=	Hour
hcp	=	Hexagonal Close Packed
HMTA	=	Hexamethylenetetramine
K	=	Kelvin
k	=	Reaction Rate Constant
K’	=	Pseudo-Reaction Rate Constant
kV	=	Kilovolts
Kα	=	K-Alpha X-Rays
La_2O_3	=	Lanthanum (III) Oxide
M	=	Molar Concentration
m^2	=	Square Meter
mA	=	Milliamps
MeOH	=	Methanol
MgO	=	Magnesium Oxide
mL	=	Milliliter

NO_x	=	Nitrogen Oxide
N_{TG}	=	Moles of Triglycerides
^oC	=	Celsius
rpm	=	Revolutions Per Minute
$-r_{TG}$	=	Rate of Triglyceride Consumption
s	=	Second
SEM	=	Scanning Electron Microscopy
SO_x	=	Sulfur Oxide
t	=	Time
TEM	=	Transition Electron Microscopy
TG	=	Triglyceride
V	=	Volume of Reaction Solution
wt%	=	Weight Percent
XRD	=	X-Ray Diffractometry
X_{TG}	=	Conversion with Respect to Triglycerides
ZnO	=	Zinc Oxide

LIST OF TABLES

TABLE I SUMMARY OF CATALYST TYPES, ADVANTAGES, AND DISADVANTAGES ... 8
TABLE II ZNO NANOROD LENGTH, WIDTH, AND ASPECT RATIO ... 27
TABLE III RELATIVE XRD PEAK INTENSITY RATIOS OF ZNO ... 33

LIST OF FIGURES

FIGURE 1- BALANCED TRANSESTERIFICATION REACTION 3
FIGURE 2- CONSECUTIVE REACTIONS INVOLVED IN TRANSESTERIFICATION 4
FIGURE 3 – WATER HYDROLYSIS TO PRODUCE FFA 5
FIGURE 4- UNDESIRABLE SAPONIFICATION SIDE REACTION 6
FIGURE 5- REACTION MECHANISM FOR BASIC METAL OXIDE CATALYZED BIODIESEL REACTION 9
FIGURE 6- HYDROLYSIS AND CONDENSATION REACTIONS TO FORM ZNO USING HMTA 12
FIGURE 7- ZNO WURTZITE UNIT CELL STRUCTURE 13
FIGURE 8 – XRD EQUIPMENT,BRUKER AXS – DIFFRAKTOMETER D8 (SERIAL NO.: 203407 KARLSRUHE, GERMANY D76181) 19
FIGURE 9 – FESEM EQUIPMENT, NOVA NANOSEM 600 FEI 20
FIGURE 10- GOLD SPUTTERING MACHINE – SPI SUPPLIES SPUTTER COATER 20
FIGURE 11-:MICROMERITICS TRISTAR 3000 POROSIMETER 21
FIGURE 12 – STAINLESS STEEL PARR INSTRUMENTS REACTOR- MODEL 4576A 22
FIGURE 13 – EPPENDORF CENTRIFUGE 23
FIGURE 14- VARIAN 400 MHZ NMR 24
FIGURE 15 – PROTONS OF INTEREST IN ^{1}H NMR ANALYSIS OF BIODIESEL SAMPLES 24
FIGURE16 – XRD PATTERN FOR SYNTHESIZED ZNO NANORODS AT DIFFERENT SYNTHESIS TIMES 27
FIGURE 17 - SEM IMAGES OF ZNO NANORODS: A) 0.5H (MAGNIFICATION 14,017X) B) 3H (MAGNIFICATION 19,058X), C) 6H (MAGNIFICATION 22,937X), D) 8H(MAGNIFICATION 14,960X), ... 28
FIGURE 18 – ZNO NANOROD YIELD WITH RESPECT TO SYNTHESIS TIME 29
FIGURE 19- BIODIESEL CONVERSION AT 150°C AT VARYING REACTION TIMES 30
FIGURE 20 – ZNO NANOROD CATALYTIC PERFORMANCE AT DIFFERENT TEMPERATURES 32
FIGURE 21- CATALYTIC PERFORMANCE COMPARISON OF ZNO: NANORODS AND CONVENTIONAL 33
FIGURE 22 – RECYCLE CATALYTIC PERFORMANCE OF THE ZNO NANORODS 34
FIGURE 23 – FIRST ORDER REACTION KINETICS AS MODELED WITH THE INTEGRAL METHOD . 36
FIGURE 24- LINEARIZATION OF REACTION KINETICS AS MODELED BY POLYNOMIAL METHOD 37
FIGURE 45
FIGURE 26 – ZNO NANOROD AND FLAKES, UREA AS AMINE PRODUCER, 64 HRS SYNTHESIS ... 46
FIGURE 27 – ZNO NANOROD, FLAKES PRODUCT AUTOCLAVE GREENE SYNTHESIS, 125°C 19H 46
FIGURE 28 – XRD PATTERN FOR CONVENTIONAL ZNO 47
FIGURE 29 – SEM IMAGE FOR CONVENTIONAL ZNO 47
FIGURE 30 – NMR SPECTRUM FOR BIODIESEL: METHOXY GROUP (SOLID BOX), METHYLENE GROUP (DASHED BOX) 48
FIGURE 31 – ZERO ORDER REACTION KINETICS FOR INTEGRAL METHOD 49
FIGURE 32 – SECOND ORDER INTEGRAL METHOD REACTION KINETICS PLOT 49
FIGURE 33 – POLYNOMIAL METHOD FIT 50

I. INTRODUCTION

Recently there has been a widespread interest and desire to become a more environmentally conscious society. This has resulted in a desire to develop renewable energy sources as well as green chemistry industrial processes. The pressure to discover an alternative to petroleum based energy has incremented with the rise in greenhouse gas emissions, environmental pollution, and the fear of exhausting oil and natural gas reserves.[1]

As scientists develop new renewable energy sources, it is vital to consider the commercialization potential of the technology. If it is to become readily available and widely used, it must be a low cost solution which requires few modifications to the existing energy infrastructure. Biodiesel is a current renewable energy source that can offer both of these characteristics.

A. Biodiesel as a Viable Alternative to Petroleum-Based Diesel

Biodiesel is a mixture of fatty acid methyl esters (FAMEs) which can be produced from the triglycerides found in animal fats and vegetable oils.[2] Biodiesel has become a very attractive alternative or supplement to petroleum based diesel since it is renewable, non-toxic, and biodegradable. In addition it has a molecular structure which contains 11-15% oxygen which increases the speed of combustion for compression ignition engines.[3]

Biodiesels also have a higher flashpoint than diesel; making storage, transportation, and handling of these fuels simpler.

While it is uncommon to find pure biodiesel for combustion engines in the market, it is not uncommon to find blends of biodiesel and petroleum diesel. The two are miscible in all proportions which provides great flexibility with respect to supply and demand.[2] Biodiesel has also been shown, either when pure or blended with petroleum diesel, to produce less CO, CO_2, and polyaromatic hydrocarbons. When pure biodiesel is used, the emissions from combustion are almost free of sulfur oxides (SO_x).[4] Unfortunately Yage et al. have found that NO_x emissions increase by 2-5% with pure biodiesel.[5]

Although his idea was not feasible until recently, Sir Rudolf Diesel (the inventor of the diesel engine) predicted that with time vegetable oil would be an important fuel. He even demonstrated this idea with peanut oil at an exhibition in Paris. [6] Since the inception of the diesel engine it has had the capability to function with oils. Currently, a blend of petroleum and biodiesel is approved for use in the vehicles of most automotive manufacturers.[7] Therefore it has been possible to implement the use of biodiesel as a fuel with minor changes to the existing infrastructure.

B. Production of Biodiesel

Attempts have been made to use pure vegetable oil for the combustion with unfavorable results. Due to the high viscosity and low volatility of pure vegetable oil the fuel lines and fuel injectors would clog and the piston heads would experience increased fouling. [1] Therefore, it is necessary to change the vegetable oil into a substance that has a

viscosity, density, and volatility similar to that of petroleum diesel. This change can be achieved through a transesterification reaction using either methanol or ethanol. This reaction is sometimes called alcoholysis.[2]

Transesterification is an equilibrium reaction which takes triglycerides, present in vegetable oil and animal fat, and methanol to produce FAMEs (fatty acid methyl esters) and glycerol. Both products in this reaction are valuable. Typically, it is necessary to have a 3:1 methanol to triglyceride stoichiometric ratio, however due to the reversibility of the reaction it is customary to have excess methanol in order to drive the reaction forward. To improve yields and reaction rate, this reaction is performed in the presence of a catalyst which can be acidic, basic, or enzymatic in nature. [1,2,7] The transesterification balanced reaction can be seen in FIGURE 1.

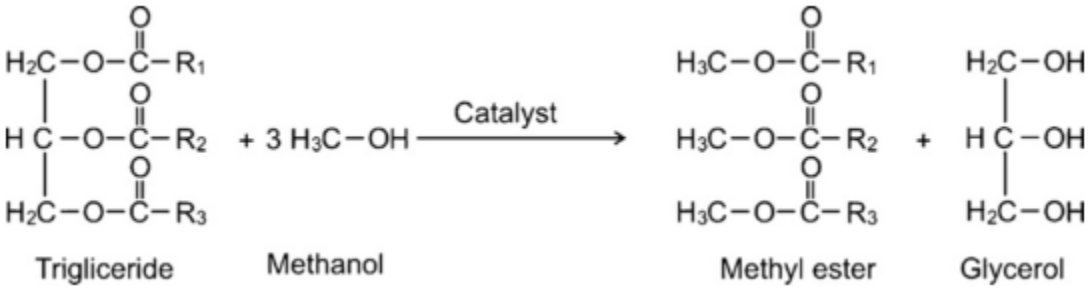

FIGURE 1- Balanced Transesterification Reaction[8]

The transesterification reaction takes place in three consecutive reversible reactions. Each reaction reduces the number of glycerides and produces one FAME. The first reaction reduces the triglycerides to a diglyceride, the second reduces a diglyceride to a monoglyceride, and the third reduces the monoglyceride to glycerol. Each of these reactions is an equilibrium reaction which favors the FAMEs and glycerol. A summary of these reactions can be seen in FIGURE 2.[2]

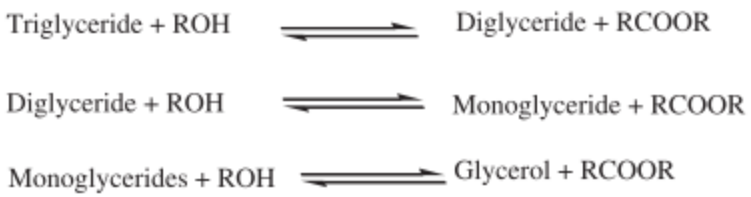

FIGURE 2- Consecutive Reactions Involved in Transesterification[9]

During the course of the reaction an immiscible layer of glycerol forms, and since it is denser than biodiesel, it sinks to the bottom of the reaction vessel. This forms a bilayer, one rich in biodiesel and one rich in glycerol. Both layers contain unreacted alcohol, oil, and catalyst and are further purified and sold.[2] As previously mentioned it is possible to use both ethanol and methanol as the alcohols for the transesterification reaction. However, it is preferred to use methanol because ethanol forms stable emulsions that make separation and purification of the phases difficult. [10]

The feedstock of triglycerides for biodiesel production generally depends on the type of oil that is readily available. It is possible to use both edible oils such as rapeseed, mustard, canola, sunflower, cotton seed, palm, soy- bean, linseed, olive, coconut, hazelnut, pistachio, sesame, safallow, and jojoba oils; as well as non-edible oils such as pongamia pinnata, jatropha and neem. These oils can also be waste cooking or frying oils. Of these feedstocks, the use of refined edible oils for biodiesel production is the least desirable because it causes a competition between production for food and fuel while simultaneously raising the costs of biodiesel. Thus, research is focusing on using non-edible oils as well as waste edible oils.[3]

The transesterification reaction only becomes a feasible way to produce biodiesel through an effective catalyst. Recent research efforts have focused both on *heterogeneous* and *homogeneous* catalysis with acidic or basic materials. The choice of catalyst for the

this reaction is heavily dependent on the moisture and free fatty acid (FFA) concentrations present in the feedstock.[11] In general, refined edible oils have much lower FFAs concentrations than non-edible oils, and waste frying and cooking oils. The moisture content of the feedstock is of vital importance since water hydrolyzes the triglycerides to produce additional FFAs. This reaction can be seen in FIGURE 3.[3]

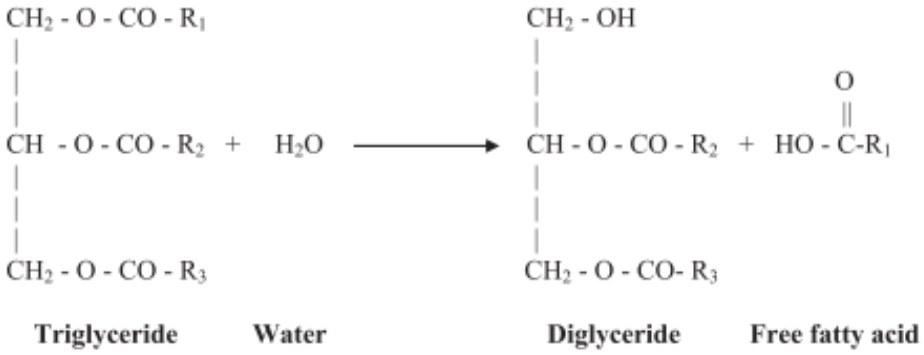

FIGURE 3 – Water Hydrolysis to Produce FFA.[3]

In general a basic catalyst is used when the FFA is up to 3 wt%, at concentrations higher than that the basic catalyst is ineffective. Acidic catalysts are used in cases with high FFA, because they can perform the esterification of the FFA as well as the transesterification of the triglycerides.[12] Although acidic catalysts are not affected by FFA concentrations, they exhibit much slower reaction rates and require higher temperatures than basic catalysts do, making basic catalysts more desirable. [1]

C. Homogeneous vs. Heterogeneous Catalysis

Currently, homogeneous catalysis is the dominant catalysis method for the production of biodiesel. It has the advantage of having faster reaction rates and low temperature requirements to produce yields of 75-98%, sometimes in as little as 30 minutes.[1] Within homogeneous catalysis, basic catalysts such as sodium hydroxide,

sodium methoxide, potassium hydroxide, and potassium methoxide are more effective than acid catalysts such as hydrochloric or sulfuric acids. Fukuda et al. report that an alkali catalyzed reaction takes place approximately 4,000 times faster than one catalyzed by the same amount of acid.[13]

Of the common homogeneous base catalysts used for this reaction, sodium hydroxide is the more prevalent since it provides high conversion rates, ease of separation, and is the least expensive of these materials.[11] However, as previously mentioned when there are oils with high FFA or moisture concentrations there is a problem with side reactions which generate FFAs and soaps. The water molecules first hydrolyze the triglyceride to generate FFAs as shown in FIGURE 3 then the homogeneous base catalyst interacts with the FFA and produces soaps as illustrated in FIGURE 4.[3]

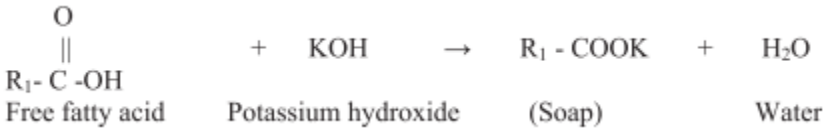

FIGURE 4- Undesirable Saponification Side Reaction [3]

Although homogeneous catalysis offers fast reaction times, high yields, and mild operating conditions, especially with alkali catalysts, it has severe drawbacks. The product effluent, a glycerol rich phase and a biodiesel rich phase contains acidic or basic catalyst which must be neutralized prior to any further purification step. Following neutralization, it is then imperative to wash both phases with water to eliminate unreacted alcohols, salts, and soap by-products. These steps add to the biodiesel processing costs as well as water utility consumption. Additionally, it is not possible to recover any of the

catalyst.[14] In order to address these drawbacks, researchers have placed a heavy focus on heterogeneous catalysis.

Heterogeneous catalysis requires that the catalyst remain in a different phase than that of the reactants, such as solid, gas, or immiscible. For the transesterification reaction, heterogeneous catalysis offers three main advantages over homogeneous catalysis: (1) the catalyst can be recycled, (2) the separation and purification of the biodiesel and glycerol products is easier due to the absence of salts and diminished soaps formation, and (3) significant reduction in the water required to wash the product phases. [8] Although heterogeneous catalysis offers several large advantages, it requires longer reaction times and harsher operating conditions to achieve the same conversions that homogeneous catalysis can achieve swiftly.[15] As with homogeneous catalysis, it is possible to have heterogeneous catalysts that are acidic or basic in nature. Among common heterogenenous catalysts are metal oxides, mixed metal oxides, zeolites, and hydrotalcites. A summary of the advantages and disadvantages of homogeneous and heterogeneous acidic or basic catalysts can be seen in TABLE I.[15]

TABLE I

SUMMARY OF CATALYST TYPES, ADVANTAGES, AND DISADVANTAGES [15]

Type	Example	Advantages	Disadvantages
Alkali			
Homogeneous	NaOH, KOH	High catalytic activity, low cost, favorable kinetics, modest operation conditions	Low FFA requirement, anhydrous conditions, saponification, emulsion formation, more wastewater from purification, disposable
Heterogeneous	CaO, $CaTiO_3$, $CaZrO_3$, CaO–CeO_2, $CaMnO_3$, $Ca_2Fe_2O_5$, KOH/Al_2O_3, KOH/NaY, Al_2O_3/KI, ETS-10 zeolite, alumina/silica supported K_2CO_3	Noncorrosive, environmentally benign, recyclable, fewer disposal problems, easily separation, higher selectivity, longer catalyst lifetimes	Low FFA requirement, anhydrous conditions, more wastewater from purification, high molar ratio of alcohol to oil requirement, high reaction temperature and pressure, diffusion limitations, high cost
Acid			
Homogeneous	Concentrated sulphuric acid	Catalyze esterification and transesterification simultaneously, avoid soap formation	Equipment corrosion, more waste from neutralization, difficult to recycle, higher reaction temperature, long reaction times, weak catalytic activity
Heterogeneous	ZnO/I_2, ZrO_2/SO_4^{2-}, TiO_2/SO_4^{2-}, carbon-based solid acid catalyst, carbohydrate-derived catalyst, Vanadyl phosphate, niobic acid, sulphated zirconia, Amberlyst-15, Nafion-NR50	Catalyze esterification and transesterification simultaneously, recyclable, eco-friendly	Low acid site concentrations, low microporosity, diffusion limitations, high cost
Enzymes	Candida antarctica fraction B lipase, Rhizomucor mieher lipase	Avoid soap formation, nonpolluting, easier purification	Expensive, denaturation

D. Metal Oxides as Heterogeneous Base Catalysts

Divalent metal oxides with covalent characters have been shown to be effective catalysts for the transesterification reaction. Metal oxides are composed of positive metal ions which act as Lewis acids and negative oxygen ions which act as Lewis bases.[9] In a mechanisms proposed by Chouhan et al. the metal oxide forms a bond with the alcohol, creating a nucleophilic oxygen on the alcohol.[8] This oxygen, then attacks the carbonyl carbon on the triglyceride which prompts the usual transesterification reaction mechanism. This process is illustrated in FIGURE 5. [8]

Among the most studied metal oxides is CaO. It offers high activity, moderate reaction conditions, and long catalyst life. In addition there are abundant sources of calcium available from egg shell and mollusk shell wastes. [16] Although it holds great catalytic promise, CaO does not offer a complete solution because it can experience strong adsorption of FFAs on the active basic sites and subsequent calcium soap

generation. It also requires thermal activation because it adsorbs CO_2 and water which poison the basic active sites, once activated it is important to work under vacuum or a nitrogen atmosphere. In addition, leaching of the Ca species reduces the reusability of the catalyst and increases processing costs. [8,16]

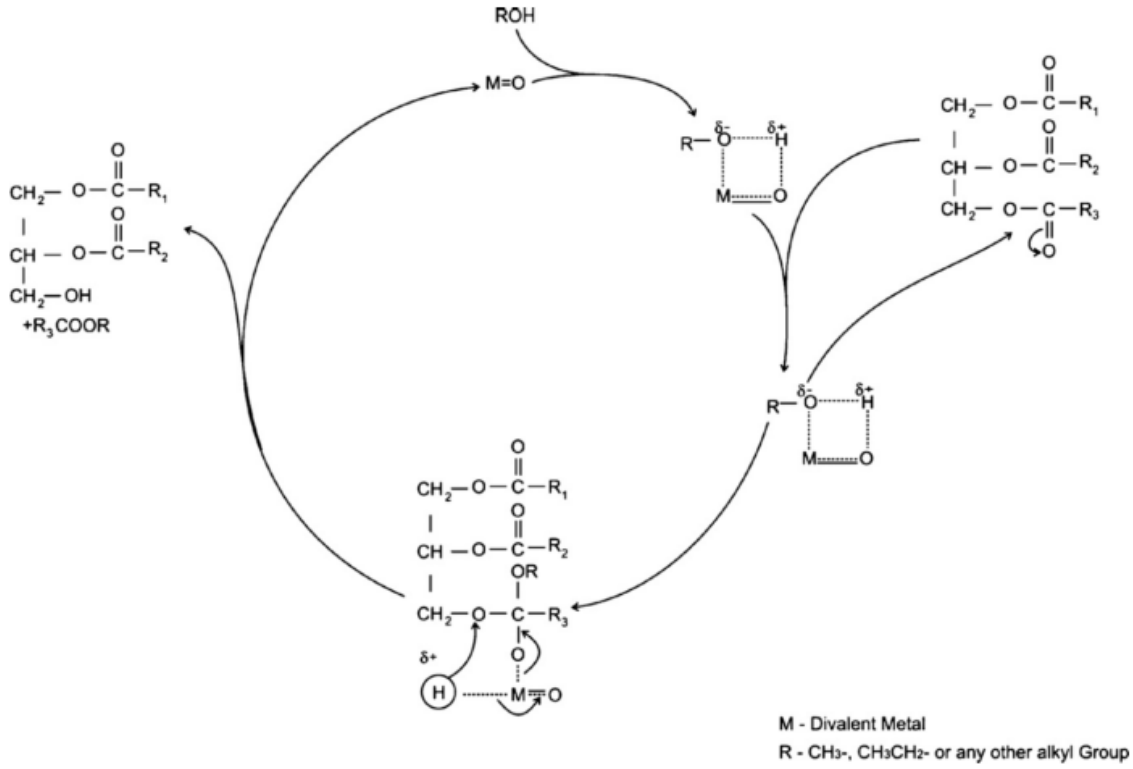

FIGURE 5- Reaction Mechanism for Basic Metal Oxide Catalyzed Biodiesel Reaction [8]

Another metal oxide that has been capable of catalyzing the transesterification reaction is MgO. Although a popular choice, it is more commonly used in combination with other metals since it has the lowest basic strength of group II oxides. This increases the basic strength of the catalyst making it more effective.[16]

It is also possible to use transition metal oxides to catalyze the transesterification reaction, and significant research has been done on ZnO. ZnO is an attractive material for

many applications because it is abundant and non-toxic.[17] Chemically it has interesting characteristics for the alcoholysis of triglycerides since it has both acidic and basic sites (Zn^{2+} acts as a Lewis acid, while O^{2-} acts as a Lewis base). Although both of these sites are weak, Bancquart et al. have shown that ZnO has an acidity/basicity ratio of 23.2.[18]

The presence of both acidic and basic sites makes ZnO a seemingly ideal catalyst for transesterification. However, this has not been shown to be the case. When compared to other metal oxides, such as CaO, MgO or La_2O_3, it demonstrated little activity as a result from its low intrinsic basicity. [18] However, a solution to improve the catalytic performance of ZnO in biodiesel production may lie with the use of nanostructures.

E. ZnO Nanostructures as Effective Catalysts for Biodiesel Production

In recent years, it has been possible to synthesize many different morphologies of nanostructures for ZnO. These have ranged from nanoparticles, nanowires, and nanobelts to nanorings, nanotubes, and nanotowers. Each structure demonstrates unique catalytic, electric, and optical properties. As these morphologies develop they expose different active planes and species.[19]

Operating on this principle Liu et al. have demonstrated that the use of nanotowers with growth in the (1 0 $\bar{1}$ 0) and (0 0 0 2) planes exposes the active O^{2-} catalytic sites. This exposure led to an increase in the biodiesel yield from 46.3% for particle like ZnO to 74.5% for the nanotower ZnO.[19] This marked improvement in conversion allows the question, is there other nanostructures that could yield higher conversions for ZnO?

F. ZnO Nanostructure Synthesis and their Catalytic Potential

ZnO nanowires and nanorods have been the subject of a widespread research push. They are commonly synthesized with gas-phase approaches such as chemical vapor deposition, pulsed laser deposition, or chemical vapor transport. With these approaches it is possible to attain single crystalline wires of several microns in length. Unfortunately, the scale-up potential for these methods is poor since they require expensive equipment, high temperatures ranging between 450-900ºC, and have low product yields. [17]

Due to these limitations, several solution approaches to ZnO nanostructure synthesis have been proposed. These solution approaches generally use a zinc salt as a zinc source coupled with an amine in an aqueous solution at temperatures ranging from 50-200ºC. The most common salts are zinc chloride ($ZnCl_2$), zinc nitrate hexahydrate ($Zn(NO_3)_2 \cdot 6H_2O$), zinc acetate ($Zn(O_2CCH_3)_2$), or zinc acetate dihydrate ($Zn(O_2CCH_3)_2 \cdot 2H_2O$) while frequently used amines include hexamethylenetetramine (HMTA), ethylenediamine (EDA), and trioctlyamine.[17,20]

The process of forming ZnO nanostructures in solution is highly sensitive to changes in pH, temperature, synthesis time, and salt counterions. To form the nanostructures the first step is to dissolve the zinc salt in water, giving rise to Zn^{2+} cations which form hydroxyl species. Depending on the pH of the solution and concentration of Zn^{2+} the predominant hydroxyl group can be $ZnOH^+(aq)$, $Zn(OH)_2(aq)$, $Zn(OH)_2(s)$, $Zn(OH)_3^-(aq)$, or $Zn(OH)_4^{2-}(aq)$. The addition of heat dehydrates these hydroxyl species and allows them to condensate, forming ZnO nuclei which serve as nucleation and growth points to develop ZnO one dimensional nanostructures.[17]

It is possible to form nanowires or nanorods in a wide range of pH ($5 < pH < 12$), however, it is simpler to form these structures at pH >9 because they can form without the presence of additives. Basic condition accelerate the synthesis because divalent metal ions dissociate with more ease under these conditions.[17] It has been proposed that amines such as HMTA are vital in the formation of ZnO nanowires and nanorods because they serve as a weak base by producing OH^- as they hydrolyze in the aqueous environment. The sequence of equilibrium reactions that takes place in the formation of ZnO from zinc salts can be seen in FIGURE 6.[21]

$$(CH_2)_6N_4 + 6H_2O \leftrightarrow 4NH_3 + 6HCHO$$

$$NH_3 + H_2O \leftrightarrow NH_3 \cdot H_2O$$

$$NH_3 \cdot H_2O \leftrightarrow NH_4^+ + OH^-$$

$$Zn^{2+} + 2OH^- \leftrightarrow Zn(OH)_2$$

$$Zn(OH)_2 \xrightarrow{\Delta} ZnO + H_2O$$

FIGURE 6- Hydrolysis and Condensation Reactions to form ZnO using HMTA[21]

The direction of the crystal growth is dependent on the adsorption of the hydroxyl species on an energetically favorable plane.[19] To understand this it is necessary to consider the crystal structure of ZnO. The typical crystal structure for ZnO is wurtzite which consists of a hexagonal unit cell with alternating layers of Zn^{2+} and O^{2-} coordinated tetrahedrally along the c-axis. An illustration of the unit cell can be seen in FIGURE 7.[21] The charge of the unit cell is neutral, however, as the crystal planes develop they can terminate with cations or anions a phenomena which yields polar surfaces.[21] Normally the [0 0 0 1] direction is the most favorable for ZnO crystal growth, but the

presence of other species such as the salt counterions, HMTA, ethylenediamine, or citric acid can cause the formation of additional energetically favorable planes thus changing the morphology of the crystal.[19]

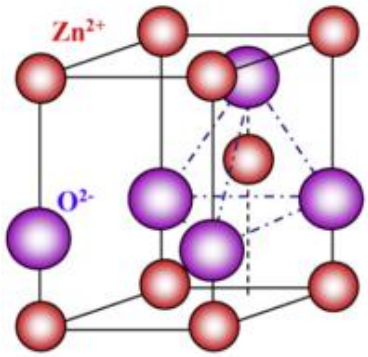

FIGURE 7- ZnO wurtzite unit cell structure [21]

Closer inspection of the ZnO wurtzite unit cell reveals that with a diameter of 0.26 nm the O^{2-} molecule is much larger than the 0.15 nm diameter of Zn^{2+}. Because of this size difference, the O^{2-} molecules are hcp while the Zn^{2+} hcp molecules occupy the interstitial tetrahedral. This results in increased exposure of the O^{2-} molecules, which are the active sites of the transesterification reaction, along the (0 0 0 2) basal plane.[19] As nanostructures develop it is possible to develop other planes that may have increased O^{2-} exposure, thus potentially increasing the catalytic activity of ZnO for the production of biodiesel.

G. Theory of Reaction Kinetics Modeling for ZnO Catalyzed Biodiesel Synthesis

Although there have been many studies of the reaction kinetics for homogeneous catalysis of the transesterification reaction, the same attention has not been paid to heterogeneous catalysis. The models that have been developed are complex and

mathematically intense and have focused mainly on MgO and CaO.[22] The heterogeneously catalyzed biodiesel synthesis is highly complex because it requires the interaction of three phases: (1) the solid catalyst, (2) the oil, and (3) the methanol.[23] The interaction between the methanol and oil is also difficult since the liquids are immiscible at room temperatures.[11]

In order to perform the kinetic analysis, simplifying assumptions, similar to those proposed by Veljković et al. were made. These assumptions are as follows: (1) the reaction takes place between the methoxide ions and triglycerides adsorbed on the catalyst surface, (2) the adsorption of the methanol on the catalyst active sites does not limit the reaction rate, (3) the mass transfer and adsorption rate of the triglycerides on the catalytic surface are initially rate limiting, (4) the desorption rate of the FAME and glycerol products does not impact the overall rate of reaction, and (5) the reaction mixture is perfectly mixed.[23]

To simplify the notation, the balanced transesterification reaction is rewritten as seen in Equation 1.[22]

$$TG + 3MeOH \overset{catalyst}{\Longleftrightarrow} 3FAME + G \tag{1}$$

Where TG is triglycerides, MeOH is methanol, FAME is fatty acid methyl esters, and G is glycerol. The differential form of the batch reactor design equation, adjusted for heterogeneous reactions, is seen in Equation 2.[24]

$$\frac{dN_{TG}}{dt} = -r_{TG}V \tag{2}$$

Where V is the reaction solution volume, N_{TG} is the number of moles of triglycerides, t is time, and r_{TG} is the rate of reaction with respect to triglycerides.

Using Equation 1 it is possible to generate a rate law for the reaction. Since there is excess methanol present in the reaction, it is assumed that reaction takes place irreversibly in the forward direction.[22] The rate law generated can be seen in Equation 3.

$$-r_{TG} = kC_{TG}^{\alpha}C_{MeOH}^{\beta} \quad (3)$$

Where k is the reaction rate constant, C_{TG} is the concentration of triglycerides, C_{MeOH} is the concentration of methanol, α is the reaction order with respect to triglycerides, and β is the reaction order with respect to methanol.

Equation 3 can be simplified by assuming the methanol is in such high excess quantities that the concentration of methanol at any point is equivalent to the initial concentration of methanol, or $C_{MeOH} = C_{MeOH,0.}$ By grouping the reaction rate constant and the concentration of methanol it is possible to create a pseudo-reaction rate constant, K', seen in Equation 4.[24]

$$K' = kC_{MeOH,0}^{\beta} \quad (4)$$

Substituting Equation 4 into Equation 3, gives the simplified rate law seen in Equation 5.

$$-r_{TG} = K'C_{TG}^{\alpha} \quad (5)$$

By using stoichiometric relations, it is possible to obtain Equation 6, where X_{TG} is the conversion with respect to oil. $C_{TG,0}$ is calculated by taking the initial moles of oil and divided by the total volume of the reaction solution.

$$C_{TG} = C_{TG,0}(1 - X_{TG}) \tag{6}$$

Combining Equation 5 with Equation 2, results in Equation 7.

$$-\frac{dC_{TG}}{dt} = K'C_{TG}^{\alpha} \tag{7}$$

By taking the natural logarithm of Equation 7 it is possible to linearize it. The linearized form can be seen in Equation 8.

$$ln\left(-\frac{dC_{TG}}{dt}\right) = \ln(K') + \alpha\ln(C_{TG}) \tag{8}$$

Knowledge of time and conversion data allows tracking of the oil concentration as a function of reaction time. Determination of the rate law parameters can then be accomplished by using Equation 8 with a plot of $\ln(C_{TG})$ vs. $ln\left(-\frac{dC_{TG}}{dt}\right)$ in the polynomial method. It is also possible to apply the integral method of rate law parameter identification. Both of these methods should be in relative agreement with each other.[24]

H. Justification

ZnO is an abundant, non-toxic material. It has both Lewis acid and Lewis base active sites which are attractive for catalysis applications. However, researchers have demonstrated that it has moderate activity and catalytic performance when it comes to the transesterification of triglycerides to produce biodiesel. The use of ZnO nanostructures has been shown to increase the catalytic performance of ZnO by providing added exposure of the O^{2-} active sites. By controlling the counterion species in ZnO nanostructure synthesis it is possible to control their morphology, and therefore the possibility to maximize the exposure of the active species and improve their catalytic performance in the transesterification reaction.

I. Objectives

1. Develop a facile, and high yield solution-synthesis approach for ZnO nanorods.
2. Propose ZnO nanorods as an effective catalyst for biodiesel synthesis.
3. Establish basic structure dependent catalytic relationships for ZnO nanorods in biodiesel synthesis.
4. Determine reaction kinetics and rate law parameters for the ZnO nanorod catalyzed biodiesel synthesis.

II. EXPERIMENTAL

A. Synthesis of ZnO Nanorods

The synthesis of ZnO nanorods was performed as reported by Greene et al. [25] In a typical synthesis, an aqueous solution of $Zn(NO_3)_2 \cdot 6H_2O$ and HMTA at a concentration of 0.025 M for both components was refluxed in a round bottom flask over a hot plate with magnetic stirring. Stirring was maintained at 300 rpm, while the temperature was held between 80-90°C. Reaction times were taken to begin when the reactant solutions were mixed, and lasted between 0.5-16 hours. As the reaction took place, ZnO crystals would precipitate from the solution. Once the reaction time was complete, the precipitate was collected using vacuum filtration and washed with DI water. The collected powder was then dried overnight.

B. Characterization of ZnO Nanorods

The ZnO nanorods were characterized using powder x-ray diffraction (XRD), field emission scanning electron miscroscopy (SEM). XRD was used to confirm the wurtzite crystalline structure of the ZnO, as well as determining the purity of the sample. The XRD equipment used is a Bruker D8-Discover diffractometer, seen in FIGURE 8, with analysis conditions at 40 kV, 40 mA with Cu Kα radiation and 2θ° from 25-90º.

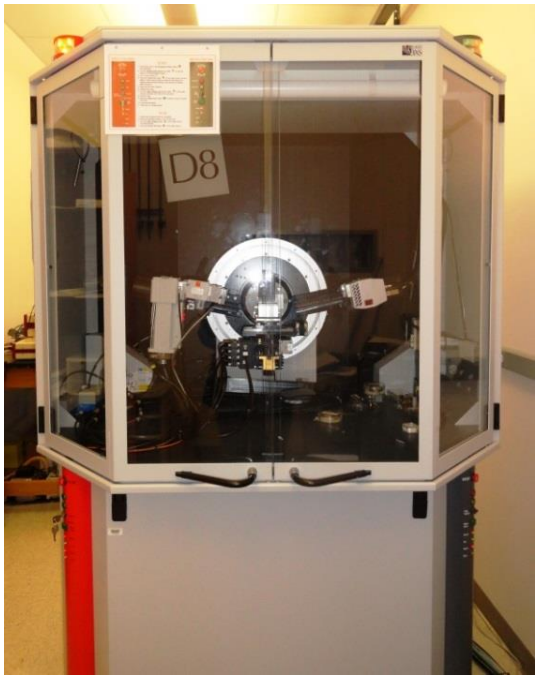

FIGURE 8 – XRD Equipment,Bruker AXS – Diffractometer D8 (Serial No.: 203407 Karlsruhe, Germany D76181)

The morphology and size of the nanorods was determined using the SEM. SEM images were collected on a Nova NanoSEM 600 FEI, which can be seen in FIGURE 9, with an acceleration voltage of 10-15 kV. Prior to SEM imaging, the samples were sputter coated with gold to prevent charging using an SPI Sputter Coater Machine, seen in FIGURE 10. The gold sputtering lasted 30 seconds.

FIGURE 9 – FESEM Equipment, Nova NanoSEM 600 FEI

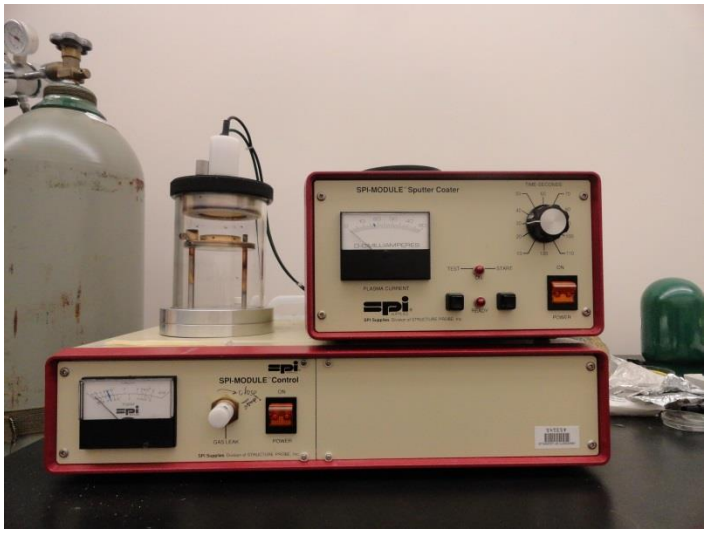

FIGURE 10- Gold Sputtering Machine – SPI Supplies Sputter Coater

(Model No. 11430, Serial No. 42345)

The BET and Langmuir surface areas of the nanorods were determined using the Micromeritics Tristar 3000 porosimeter seen in FIGURE 11. The conditions on the

porosimeter were a temperature of 77 K using liquid nitrogen as a coolant. The samples were degassed at 160 °C for four hours directly before being placed in the porosimeter.

FIGURE 11-:Micromeritics Tristar 3000 Porosimeter

C. Biodiesel Synthesis and Characterization

The transesterification reactions were carried out in a 250 mL stainless steel high pressure Parr reactor seen in FIGURE 12. Each reaction was performed with a 50:1 molar ratio of methanol to oil and a catalyst concentration of 1-8 wt% of oil. The feedstock for the transesterification reaction was extra virgin cold pressed olive oil. The methanol was purchased from Acros Organics (99% purity) and was used without further processing. The catalysts were the as synthesized ZnO nanorods.

FIGURE 12 – Stainless Steel Parr Instruments Reactor- Model 4576A

In a typical reaction 0.05 g of ZnO nanorods, 5 mL of olive oil, and 30 mL of methanol were placed in the stainless steel reactor. The reactor was then pressurized to 4 bar with argon gas to create an inert atmosphere. The resulting mixture was then continuously stirred and heated to 120, 150, or 180°C. The reaction time ranged between 0.5 – 8 hours and was begun as soon as the thermocouple registered the desired reaction temperature. Once the reaction time was complete, the reactor was cooled using an ice bath.

The reactor effluent was centrifuged for three minutes at 4,000 rpm in an Eppendorf centrifuge seen in FIGURE 13. The supernatant was collected and placed in an oven to remove the excess methanol. The spent ZnO nanorod catalyst was washed

with acetone twice and dried in the oven overnight. The spent catalyst was characterized using the same methods and equipment used to characterize the fresh ZnO nanorods.

FIGURE 13 – Eppendorf Centrifuge

Model No.5702 Serial No. 5702YN320989

The biodiesel conversion was quantified using proton nuclear magnetic resonance (^{1}H NMR). After the excess methanol evaporates two phases remain: the top phase is rich in biodiesel while the denser bottom layer is rich in glycerol. Samples from the top layer were taken, placed in deuterated chloroform (Cambridge Isotope Laboratories, Inc. 99.8%) and then analyzed in a Varian 400 MHz NMR seen in FIGURE 14.

FIGURE 14- Varian 400 MHz NMR

The ^{1}H NMR provides a spectrum of chemical shifts belonging to the protons present in the sample. To quantify the reaction progress there are two peaks of interest, the peak belonging to the methylene group adjacent to the carbonyl group in triglycerides (seen at 2.3ppm) and the methoxy group in FAMEs (seen at 3.7 ppm).[2] The location of these two groups in the molecules of interest can be seen in FIGURE 15.

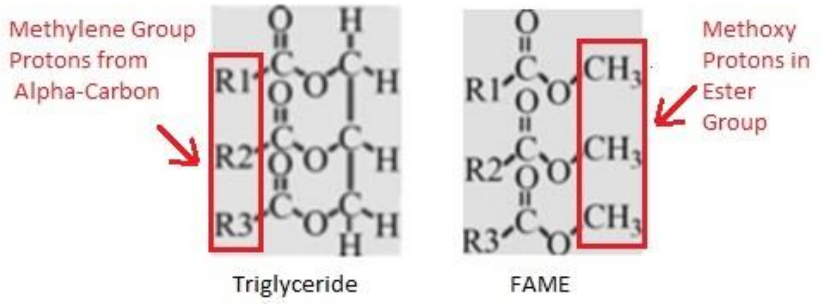

FIGURE 15 – Protons of Interest in ^{1}H NMR Analysis of Biodiesel Samples

The three protons on the methoxy group in the FAME molecule are present only in FAME products so their signal serves to quantify the conversion. Meanwhile, the two protons for the methylene group of the triglycerides are present both in the reactants and the products so they serve as the baseline for comparison of the new products. By determining the area of the peaks generated by these protons it is possible to quantify analytically the conversion achieved. A mathematical expression to calculate the conversion can be seen in Equation 1.

$$X = \frac{2A_{\text{Methoxy Proton}}}{3A_{\alpha-\text{Carbon Proton}}} \quad (1)$$

A representative ^{1}H NMR spectrum can be seen in the Appendix.

III. RESULTS AND DISCUSSION

A. ZnO Nanorod Solution Synthesis and Characterization

The ZnO nanostructure synthesis method developed by Greene et al. was followed closely with a few variations to determine the parameters which provided the highest product yield. [25] These variations included decreasing the synthesis temperature, changing the synthesis time, the use of hydrothermal treatment in a Teflon lined autoclave, and substituting ethylenediamine and urea instead of HMTA. All of these reaction conditions produced ZnO with a wurtzite crystal structure as confirmed by XRD. However, only the change in temperature and synthesis time yielded nanostructures with a consistent and desirable morphology, nanorods. SEM images of the other synthesis conditions can be seen in the Appendix.

The synthesis time was varied from 0.5-16.5 hours. The XRD patterns corresponding to each synthesis time are in agreement with the relative peak positions and intensity of the wurtzite crystal structure (JCPDS pattern 01-075-0576).[17] These diffraction patterns can be seen in FIGURE 16. The intensity of the primary peaks in the XRD spectrum increased with longer synthesis times. This indicates that longer synthesis times result in an added degree of crystallinity of the material.

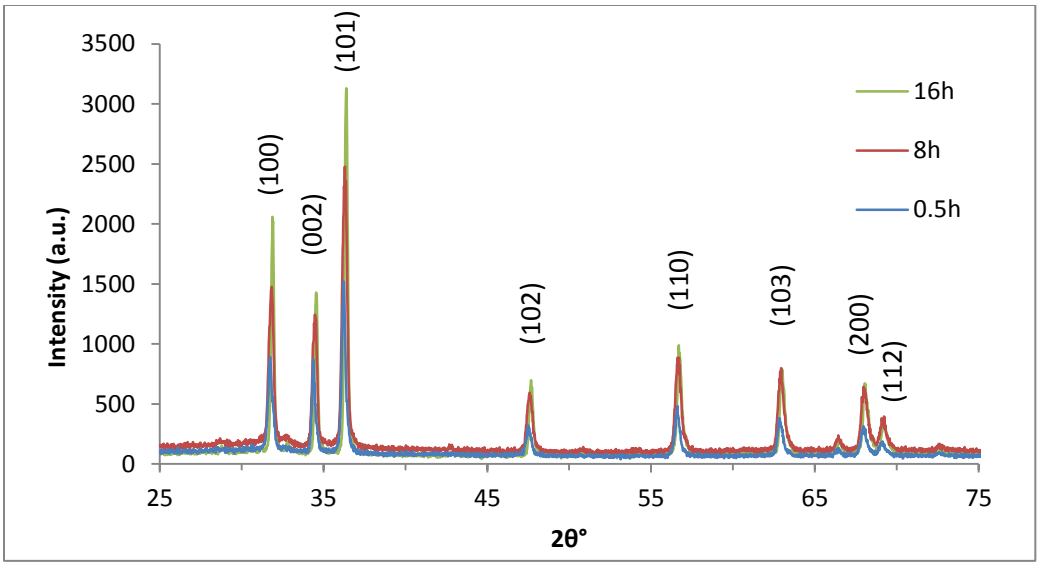

FIGURE16 – XRD Pattern for Synthesized ZnO Nanorods at Different Synthesis Times

The morphology of the synthesized material can be seen in the SEM images found in FIGURE 17 Comparison of these images reveals that there is no apparent trend in terms of length as a function of time. However, it can be noted that the diameter of the nanorods becomes very large at long synthesis times. This data can be seen in Table II. In general, it appears that increasing synthesis time provides an increase in variation of the aspect ratios.

TABLE II

ZNO NANOROD LENGTH, WIDTH, AND ASPECT RATIO

Time (h)	Average Length (µm)	Average Width (µm)	Average Aspect Ratio
0.5	2.99 ± 1.01	0.67 ± 0.19	4.62 ± 1.65
3	4.76 ± 2.95	0.77 ± 0.45	6.35 ± 1.90
6	1.48 ± 0.35	0.41 ± 0.07	3.61 ± 2.21
8	2.27 ± 0.40	0.51 ± 0.12	4.53 ± 0.72
16.5	3.11 ± 0.93	0.80 ± 0.54	5.98 ± 3.73

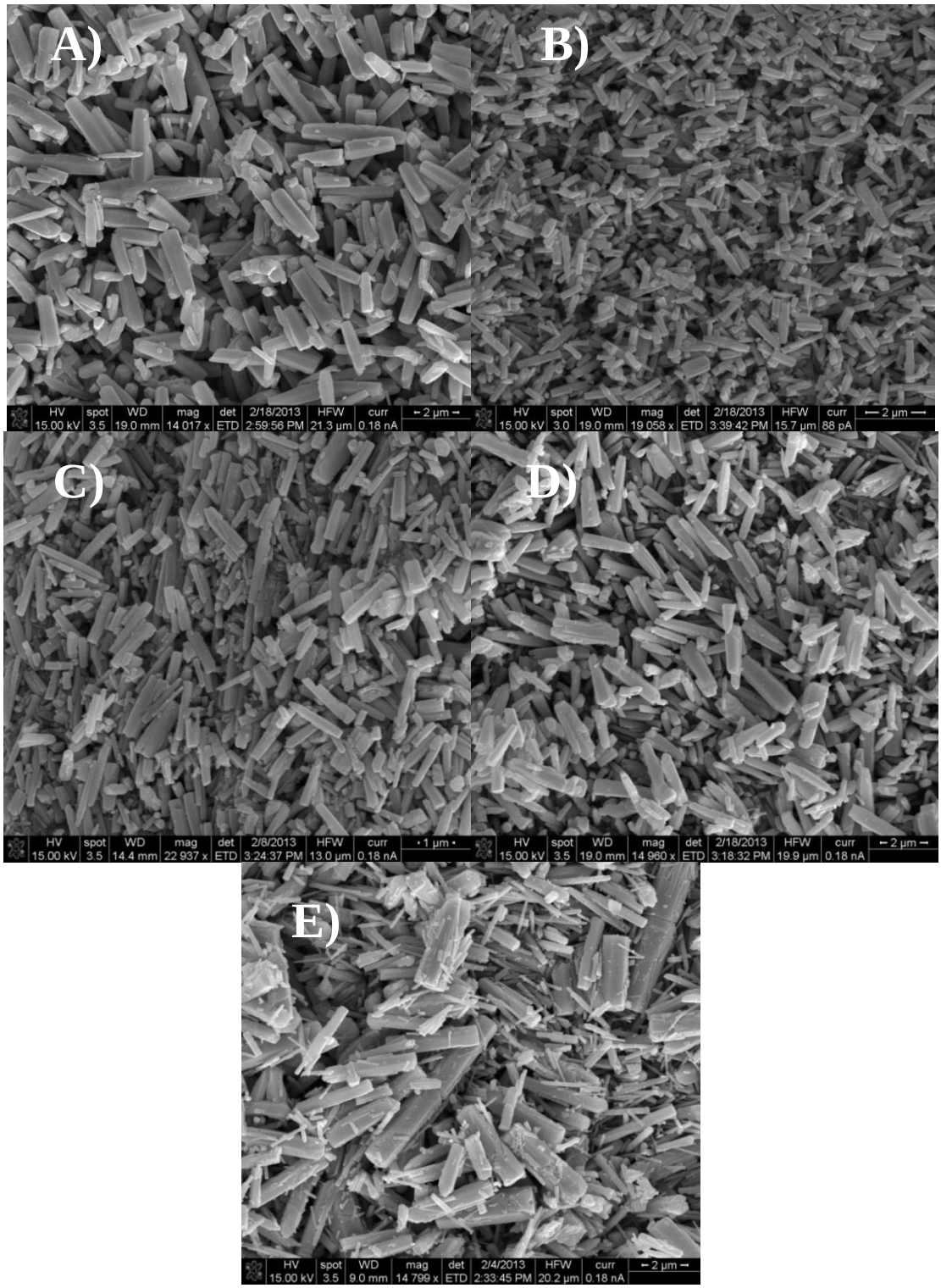

FIGURE 17 - SEM Images of ZnO Nanorods: A) 0.5h (magnification 14,017x) B) 3h (magnification 19,058x), C) 6h (magnification 22,937x), D) 8h (magnification 14,960x), E) 16.5h (scale 2μm, magnification 14,799x)

From the data it is also possible to determine that ZnO nanorod yield is a function of time. As seen in FIGURE 18, nanorod yield is asymptotic in nature. After three hours of synthesis time, there is no noticeable increase in the nanorod yield.

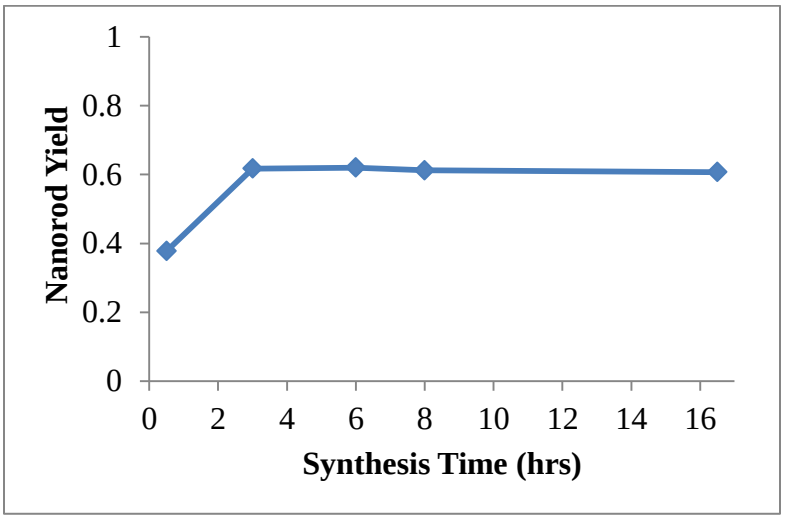

FIGURE 18 – ZnO Nanorod Yield with Respect to Synthesis Time

This phenomenon stems from the growth mechanism of the ZnO nanorods. In the formation of the nanorods, the $Zn(NO_3)_2 \cdot 6H_2O$ must be hydrolyzed, and then condensed. As it condenses ZnO nuclei are formed which must surpass the minimum nuclei size if the crystal is to grow. Once the minimum nuclei size has been surpassed, the crystal grows in the [0 0 0 1] direction.[17] However, there is also radial growth and with increasing synthesis times the nanorods exhibit larger diameters as the material begins to synterize. [25]

Comparison of this growth mechanism with FIGURE 18 indicates that from 0.5-3 hours of synthesis time, there is still formation of ZnO nuclei and therefore nanorod formation. After three hours no new nuclei are formed and the rods fuse together, leaving the yield stagnant.[25] This can also be confirmed visually in FIGURE 17. Greene et. al

increased the length of the rods by introducing a fresh solution of reactants, there were no attempts to do so in this work.[17]

Based on the results, the nanorods produced after three hours of synthesis time were of high quality and high percent yield, and were used in the biodiesel catalysis studies. The BET surface area of these nanorods was found to be 0.3204 m^2/g.

B. ZnO Nanorods as Catalysts for Biodiesel Production

The ZnO nanorods were used in a 1wt% of oil concentration to catalyze the transesterification reaction from olive oil to biodiesel. The reactions were run at 150ºC and different reaction times. The results are plotted in FIGURE 19, were a sigmoidal curve is apparent. The highest conversion, 94.8%, was obtained at eight hours of reaction time. This demonstrates that ZnO nanorods can serve as an effective catalyst for biodiesel synthesis.

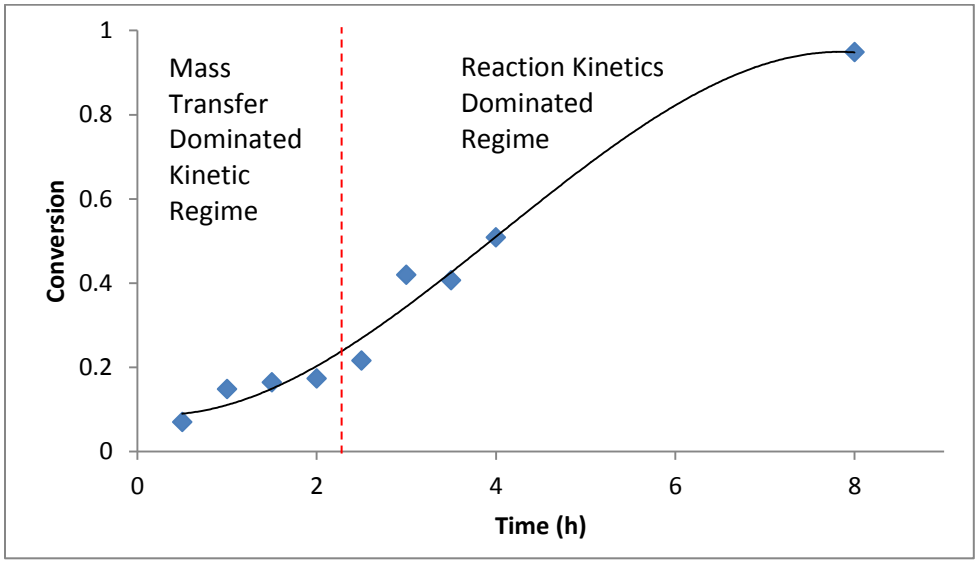

FIGURE 19- Biodiesel Conversion at 150ºC at Varying Reaction Times

Initially the reaction takes place slowly with low conversions. This is caused by the strong mass transfer limitations that are inherent in the system. The system is made up of three phases: liquid methanol phase, liquid oil phase, and the solid catalyst phase.[26] So, initially it is imperative that all phases mix well by using continuous stirring during what can be considered an adaptation phase. During this adaptation phase an emulsion of the phases is generated and the reaction rate increases.[11] Once the reaction time reached 2.5 hours the reaction rate and conversion incremented quickly. The shape of the curve may also be a product of the increased solubility of the methanol phase in the oil and FAME mixture as FAMEs are produced, which reduces the mass transfer limitations.[23]

Bancquart et al. demonstrated that ZnO has an intrinsic basicity of 22 μmol/g and an intrinsic acidity of 455 μmol/g, provided by O^{2-} and Zn^{2+} molecules respectively. [18] It has been well documented that the ZnO active sites for this reaction are the O^{2-} molecules[19]. ZnO catalyzes the reaction by forming weak bonds with the methanol. The O^{2-} forms bonds with the H^{+} in the methanol while the metal forms a weak bond with the resulting methoxy group. The methoxy group then attacks the carbonyl group in the triglyceride molecule and begins the transesterification process.[26]

The effect of temperature on catalyst performance was also studied, by running reactions at different temperatures for three hours for ease of comparison. The results can be seen in FIGURE 20. It is apparent that higher temperatures yield higher biodiesel conversions, which is in accordance to literature reports for biodiesel synthesis. [27] A maximum conversion of 87.0% at three hours was obtained with a temperature of 180ºC. However, in the interest of energy conservation, it is desired to use reaction conditions

that are milder in nature. Therefore since the ZnO nanorods demonstrated adequate catalytic activity at 150°C, all subsequent studies were performed at this temperature.

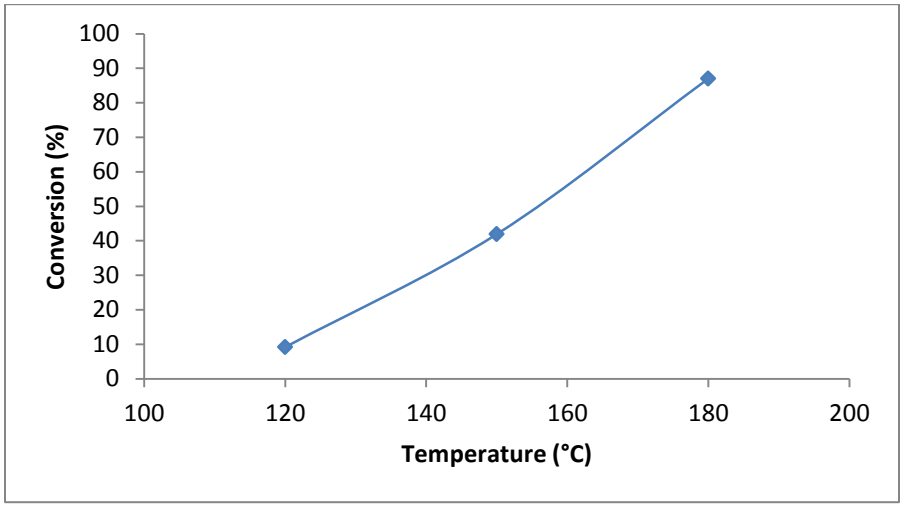

FIGURE 20 – ZnO Nanorod Catalytic Performance at Different Temperatures

In order to provide a comparison of the ZnO nanorod catalytic activity, ZnO with no apparent morphology was synthesized by calcining $ZnCO_3$ basic (Sigma Aldrich, 58% Zn) at 450ºC for four hours. The material was characterized in the same way the ZnO nanorods were, XRD patterns and SEM images can be seen in the Appendix. It displayed a wurtzite crystal structure, and a BET surface area of 15.9446 m^2/g. The catalytic performance of the ZnO was then tested by running a reaction at 150ºC for eight hours and compared to that of the ZnO nanorods, the results can be seen in FIGURE 21.

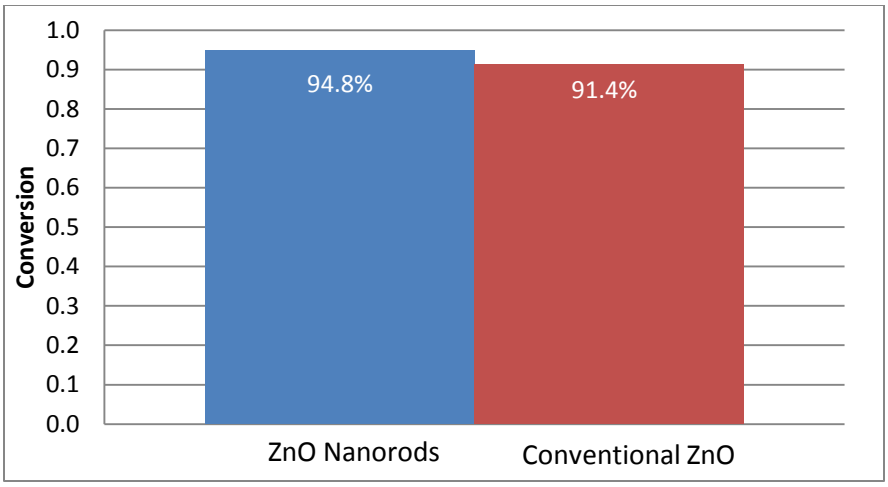

FIGURE 21- Catalytic Performance Comparison of ZnO: Nanorods and Conventional

The catalytic performance of the ZnO nanorods was slightly better than that of the conventional ZnO. The improvement in catalytic activity can be attributed in part to the increased degree of crystallinity of the wurtzite crystal structure primary planes (101), (100), and (002) in the ZnO nanorods. Comparison of the primary peaks in the XRD patterns for both materials, confirms the increased degree of crystallinity of the ZnO nanorods. Ratios of the intensity of the peaks (nanorods/conventional) can be seen in Table III. The improved crystallinity in the (002) basal plane provides increased exposure of the lattice oxygens (O^{2-}) of the ZnO considered as the active sites for transesterification reactions.[19]

TABLE III

RELATIVE XRD PEAK INTENSITY RATIOS OF ZNO

Peak	Intensity Ratio (Nanorod/Conventional)	Intensity Ratio (Fresh/Spent)	Intensity Ratio (Fresh/Recycle)
(100)	1.11	1.44	2.04
(002)	1.20	1.63	2.45
(101)	1.18	1.45	2.12

The reusability of the catalyst was also investigated. The spent catalyst from the eight hour reaction time at 150ºC was characterized and calcined at 450ºC for five hours prior to undergoing another reaction at the same operating conditions. The results can be seen in FIGURE 22. The conversion of the recycled catalyst was 77.4% compared to that of the fresh catalyst, 94.1%. This indicates a deactivation of 18.4%.

This deactivation was a result of a marked loss in degree of crystallinity of the catalyst. The ratios of the peak intensity of the fresh, spent (one reaction cycle), and recycled (two reaction cycles) catalysts can be seen in Table III. The relative ratios of the fresh, spent, and recycled catalyst increased. This increase, indicates decreased degree of crystallinity of the spent and recycled material compared to the fresh material. Because part of the increased activity of the ZnO nanorods is derived from the added exposure the O^{2-} molecules have in the (0 0 2) plane, such a large loss in degree crystallinity has a profound impact on the catalytic performance of the material. In addition, the loss of catalytic activity in the recycled catalyst may be also related to the presence of unremoved carbonaceous species formed during the transesterification reaction.

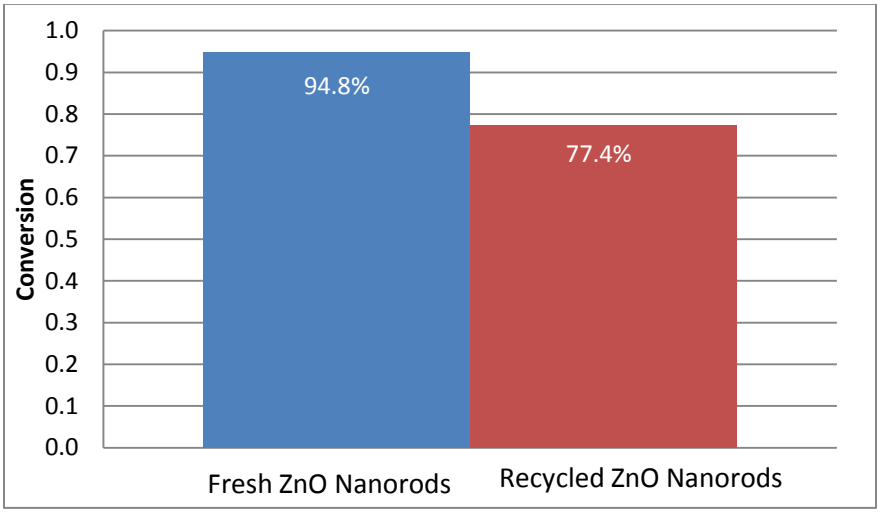

FIGURE 22 – Recycle Catalytic Performance of the ZnO Nanorods

C. Reaction Kinetics of the ZnO Nanorod Catalyzed Biodiesel Reaction

The reaction kinetics of the ZnO nanorod catalyzed reaction were determined by using the integral method and polynomial methods. To apply these methods, the data points from 0-2 hours of reaction time were ignored. As previously discussed, this is the adaptation period for the reaction in which triglyceride mass transfer limitations control the kinetics of the reaction.[23] Thus their inclusion would not be representative of the surface reaction kinetics.

From the integral method, it was determined that the reaction was of first order with respect to oil. The plot of time vs $\ln(C_{TG})$ and corresponding linear fit can be seen in FIGURE 23. The plots that correspond to zero and second order reaction kinetics can be seen in the Appendix. The linearization obtained from FIGURE 23 can be seen in Equation 9.

$$ln(C_{TG}) = \ln\left(C_{TG,0}\right) - K't = -6.5896 - 0.5136t \quad (9)$$

Using Equation 9, a pseudo reaction constant of 0.5136 h^{-1} was calculated. Equation 9 also predicts an initial C_{TG} of 0.001375 $\frac{mol\ TG}{mL\ solution}$. This value is a slight over estimate of this concentration since the reactor was fed 0.000412 $\frac{mol\ TG}{mL\ solution}$.

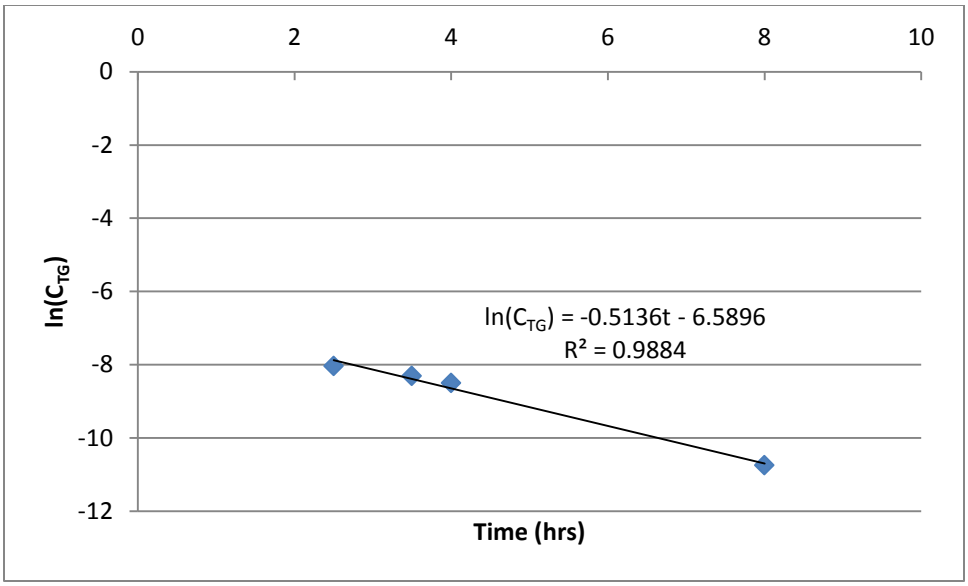

FIGURE 23 – First Order Reaction Kinetics as Modeled with the Integral Method

The kinetics of the reaction were also modeled using the polynomial method. The plot of C_{TG} vs time can be seen in the Appendix. The trend line obtained from this plot can be seen in Equation 10.

$$C_{TG} = 0.000006t^2 - 0.0001t + 0.006 \quad (10)$$

$$R^2 = 0.9997$$

Equation 10 was then used in conjunction with Equation 8 to generate the plot depicted in FIGURE 24. The linearization obtained from FIGURE 24 can be seen in Equation 11.

$$\ln\left(-\frac{dC_{TG}}{dt}\right) = 1.0845\ln(C_{TG}) - 0.7513 \quad (11)$$

$$R^2 = 0.9959$$

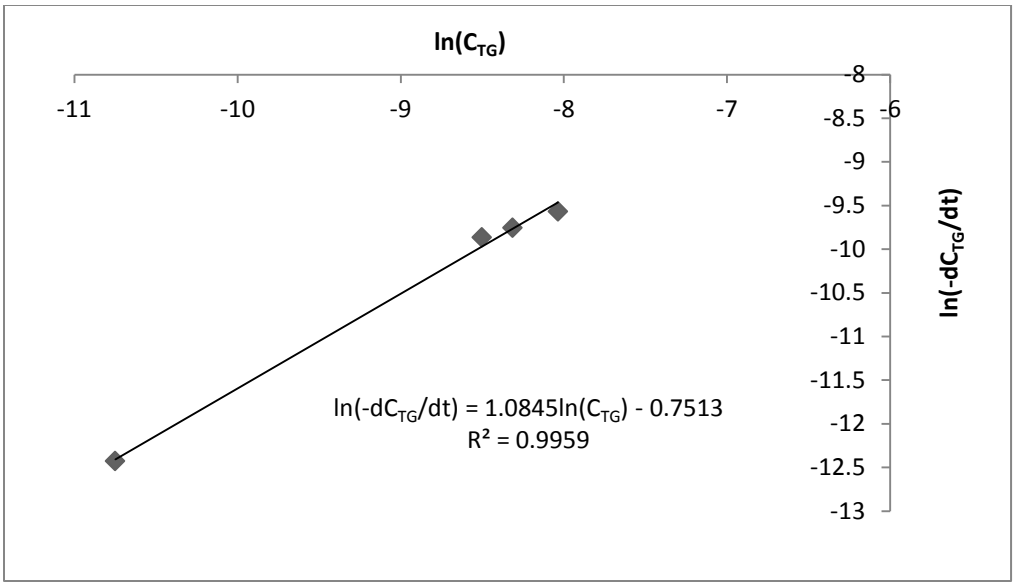

FIGURE 24- Linearization of Reaction Kinetics as Modeled by Polynomial Method

The obtained linearization translates to a reaction order of 1.0845 with respect to the triglycerides. This value corresponds to that reported by Ilgen et al. for the transesterification of canola oil using a KOH/MgO catalyst system. [22] A pseudo reaction rate constant of 0.4717 $\frac{1}{h}\left(\frac{ml}{mol\ TG}\right)^{(1-\alpha)}$ was also obtained. Comparison with the reaction rate constant reported by Ilgen et al. revealed that the reaction constant for nanorod system is larger, yet they are of the same order of magnitude. The discrepancy is caused by the use of different catalyst, reaction temperatures, and oil feedstocks.

The kinetic model obtained by the polynomial method demonstrates good agreement with that obtained by the integral method. The pseudo reaction rate constants are within 8% of each other. The order of reaction with respect to triglycerides also demonstrated good agreement since the polynomial method can be described as pseudo first order kinetics.

This behavior is not uncommon, Kouzo et. al reported that a CaO catalyzed biodiesel reaction using soybean oil fluctuated from zero order to first order as the reaction progressed and FAMEs were formed. [28] There have also been many reports using metal oxides such as CaO and MgO that catalyzed biodiesel is first order with respect to the triglyceride. [11,13,22,23,27]

IV. CONCLUSIONS

ZnO nanorods were successfully synthesized using the solution method approach developed by Greene et al. Comprehensive materials characterization was performed by using XRD, FESEM, and a porosimeter to determine the BET surface area. From the study to determine the effect of synthesis time on the nanorod morphology it is demonstrated that with increasing synthesis times, the crystallinity of the material increases. The average length of the nanorods remained the same regardless of the synthesis time, however, the aspect ratio demonstrated increased variation with increasing synthesis times.

The percent yield of nanorods was deeply affected by the synthesis time, demonstrating asymptotic behavior with respect to time. This phenomenon was caused by the rate of hydrolysis and condensation of the $Zn(NO_3)_2 \cdot 6H_2O$ salt. ZnO nuclei are being formed until the synthesis time reaches three hours, at which point the formation of new nuclei is diminished and the nanorods begin to fuse together.

The catalytic performance of the ZnO nanorods in the production of biodiesel was good. The study to determine the effect of reaction time on the conversion demonstrated that mass transfer limitations between the two liquid phases and solid catalysts were dominant and diminished the conversion achieved at low synthesis times. However it was possible to achieve a conversion of 94.8% after eight hours of reaction time at 150ºC. A

temperature study was also conducted for a reaction time of three hours which revealed that with increasing temperature it is possible to achieve higher conversions.

The reusability of the ZnO nanorods was also studied. After two reaction cycles there was a marked loss in crystallinity which resulted in lower conversions. Comparison studies with conventional ZnO at the same reaction conditions demonstrated that the ZnO nanorods had better catalytic performance at 150ºC for eight hours of synthesis time. The improved catalytic performance is contributed to improved crystallinity of the (0 0 2) basal plane, thus exposing O^{2-} active sites.

From the kinetic study it was determined that the pseudo reaction rate constant was 0.5136 h^{-1} with a pseudo-first order rate of reaction with respect to triglycerides. Due to this the rate of reaction shows some dependence on the concentration of triglycerides present in the reaction mixture.

VI. RECOMMENDATIONS

A. ZnO Nanorod Synthesis and Catalytic Potential for Biodiesel Production

The synthesis of ZnO nanorods took place under mild conditions and had relatively high nanorod yields. However, their aspect ratio was low. The addition of fresh precursor solution at three hours of synthesis time could increase their length. This could provide added crystalline order or surface area, thus enhancing the catalytic properties of the material. It might also be of interest to explore other nanostructures such as nanotubes since the hollow structure would provide added surface area. Additional surface area may help increase the catalytic activity of the material and reduce the reaction time required to achieve high biodiesel yields.

B. ZnO Nanorod Characterization

Additional characterization techniques can be used to further investigate the crystalline structure of the ZnO nanorods. The use of transmission electron miscroscopy (TEM) would be helpful in obtaining detailed crystallographic information. This information would be valuable in confirming the added exposure of the O^{2-} active sites of the biodiesel reaction.

C. ZnO Nanorods Catalyzed Biodiesel Synthesis Kinetics

The effect of a solvent such as tetrahydrofuran or dimethylsulfoxide should be studied. These solvents have been known to increase the solubility of the oil and methanol, which has the potential to reduce mass transfer limitations. This would help improve reaction times.

The catalytic activity of the nanorods should also be studied using a more common oil feedstock. Olive oil was used because of the ready availability it has. However, for a more scalable operation oil feedstocks such as waste frying oils should be used.

Additional studies should be conducted to develop a more detailed kinetic model based on Eley-Rideal or Langmuir-Hinshelwood mechanisms. Inclusion of the mass transfer limitations caused by the adsorption of the triglyceride on the catalyst surface in the kinetic study would aid in obtaining a complete understanding of the potential of ZnO nanorods to become a feasible scale up catalyst.

VII. REFERENCES

(1) Shahid, E. M.; Jamal, Y. *Renewable and Sustainable Energy Reviews* **2011**, *15*, 4732–4745.

(2) Tariq, M.; Ali, S.; Khalid, N. *Renewable and Sustainable Energy Reviews* **2012**, *16*, 6303–6316.

(3) Atadashi, I.; Aroua, M. *Journal of Industrial and …* **2012**, *19*, 14–26.

(4) Sahoo PK, Das LM, Babu MKG, N. S. *Fuel* **2007**, *86*.

(5) Yage D, Cheung CS, H. Z. *Sci Total Environ* **2009**, *40*.

(6) Orchard B, Jon D, J. C. *World Pumps* **2007**, *24*.

(7) Semwal, S.; Arora, A. K.; Badoni, R. P.; Tuli, D. K. *Bioresource technology* **2011**, *102*, 2151–61.

(8) Chouhan, a. P. S.; Sarma, a. K. *Renewable and Sustainable Energy Reviews* **2011**, *15*, 4378–4399.

(9) Zabeti, M.; Wan Daud, W. M. A.; Aroua, M. K. *Fuel Processing Technology* **2009**, *90*, 770–777.

(10) Zhou W, Konar SK, B. D. *J Am Oil Chem Soc* **2003**, *80*.

(11) Meher, L.; Vidyasagar, D.; Naik, S. *Renewable and Sustainable Energy Reviews* **2006**, *10*, 248–268.

(12) JV., G. *Fuel Process Technol* **2006**, *86*, 107.

(13) Fukuda, H.; Kondo, a; Noda, H. *Journal of bioscience and bioengineering* **2001**, *92*, 405–16.

(14) Tariq, M.; Ali, S.; Khalid, N. *Renewable and Sustainable Energy Reviews* **2012**, *16*, 6303–6316.

(15) Leung, D. Y. C.; Wu, X.; Leung, M. K. H. *Applied Energy* **2010**, *87*, 1083–1095.

(16) Borges, M. E.; Díaz, L. *Renewable and Sustainable Energy Reviews* **2012**, *16*, 2839–2849.

(17) Greene, L. E.; Yuhas, B. D.; Law, M.; Zitoun, D.; Yang, P. *Inorganic chemistry* **2006**, *45*, 7535–43.

(18) Bancquart, S.; Vanhove, C.; Pouilloux, Y.; Barrault, J. **2001**, *218*, 1–11.

(19) Liu, F.; Zhang, Y. *Ceramics International* **2011**, *37*, 3193–3202.

(20) Akgun, M. C.; Kalay, Y. E.; Unalan, H. E. *Journal of Materials Research* **2012**, *27*, 1445–1451.

(21) Wang, Z. L. *Materials Science and Engineering: R: Reports* **2009**, *64*, 33–71.

(22) Ilgen, O.; Akin, A. N. *"Applied Catalysis B, Environmental"* **2012**, *126*, 342–346.

(23) Veljkovic, V. B.; Stamenkovic, O. S.; Todorovic, Z. B.; Lazic, M. L. *Fuel* **2009**, *88*, 1554–1562.

(24) Fogler, H. S. *Elements of Chemical Reaction Engineering*; 4th ed.; Prentice Hall, 2010; pp. 253–291.

(25) Greene, L. E.; Law, M.; Goldberger, J.; Kim, F.; Johnson, J. C.; Zhang, Y.; Saykally, R. J.; Yang, P. *Angewandte Chemie (International ed. in English)* **2003**, *42*, 3031–4.

(26) Endalew, A. K.; Kiros, Y.; Zanzi, R. *Biomass and Bioenergy* **2011**, *35*, 3787–3809.

(27) Jain, S.; Sharma, M. P. *Bioresource technology* **2010**, *101*, 7701–7706.

(28) Kouzu M, Kasuno T, Tajika M, Sugimoto Y, Yamanaka S, H. J. *Fuel* **2008**, *87*.

VIII. APPENDIX: SUPPORTING INFORMATION

A. Alternative ZnO Nanorod Synthesis Methods

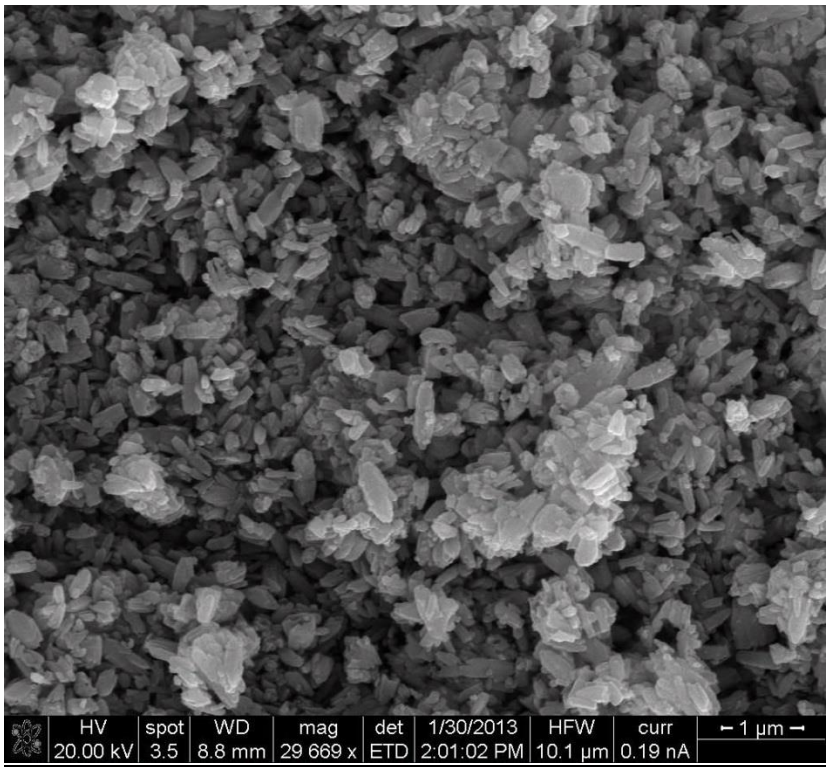

FIGURE 25 – ZnO Nanoplates Obtained using EDTA Instead of HMTA, Three Hours Synthesis Time

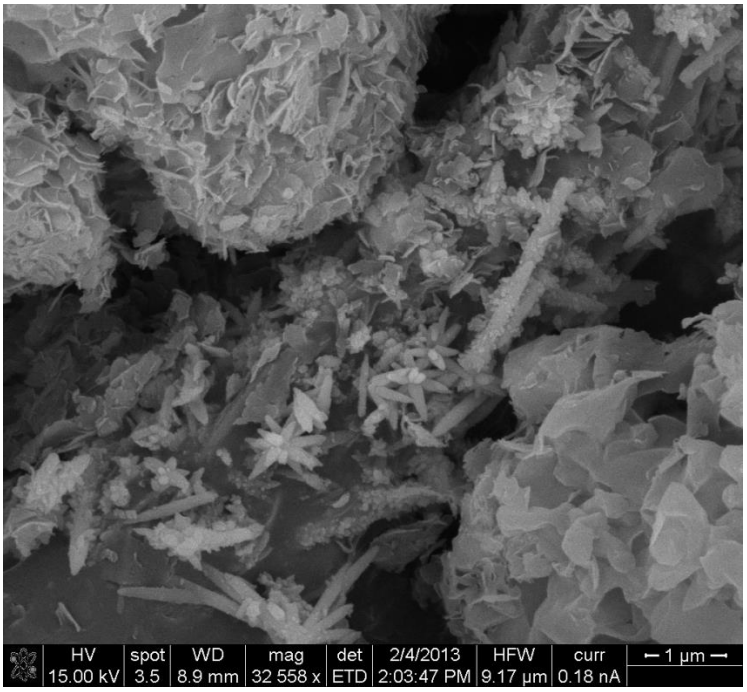

FIGURE 26 – ZnO Nanorod and Flakes, Urea as Amine Producer, 64 hrs Synthesis

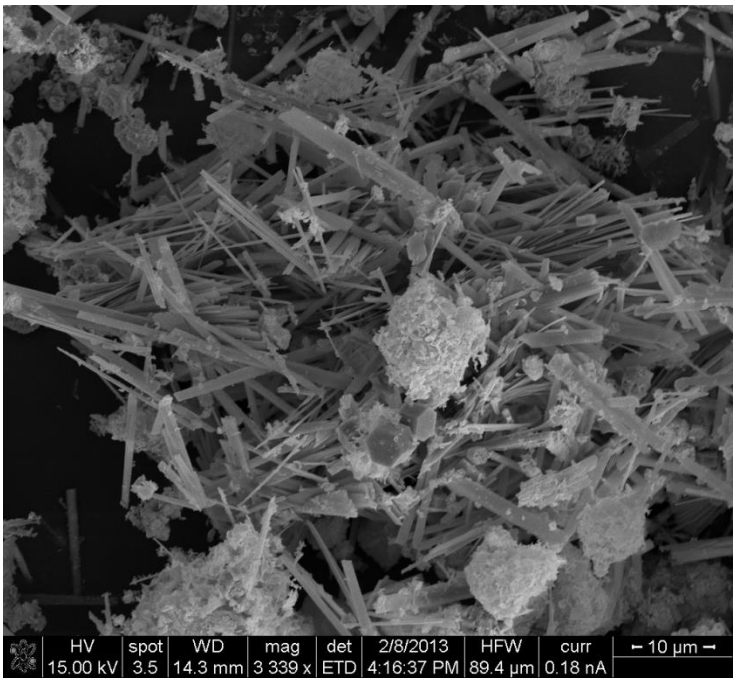

FIGURE 27 – ZnO Nanorod, Flakes Product Autoclave Greene Synthesis, 125ºC 19h[25]

B. Materials Characterization for Conventional ZnO

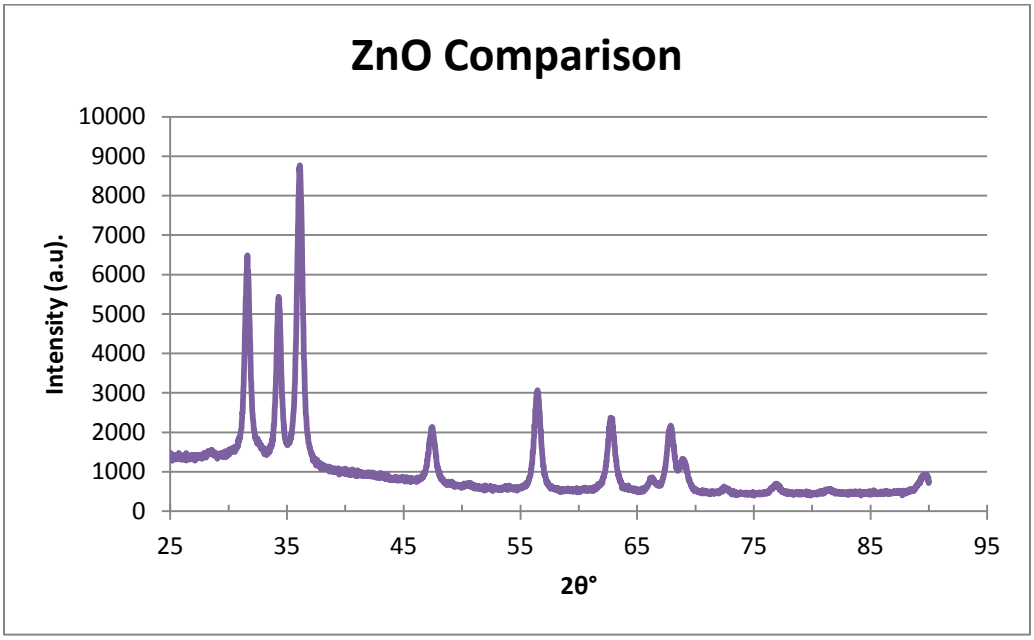

FIGURE 28 – XRD Pattern for Conventional ZnO

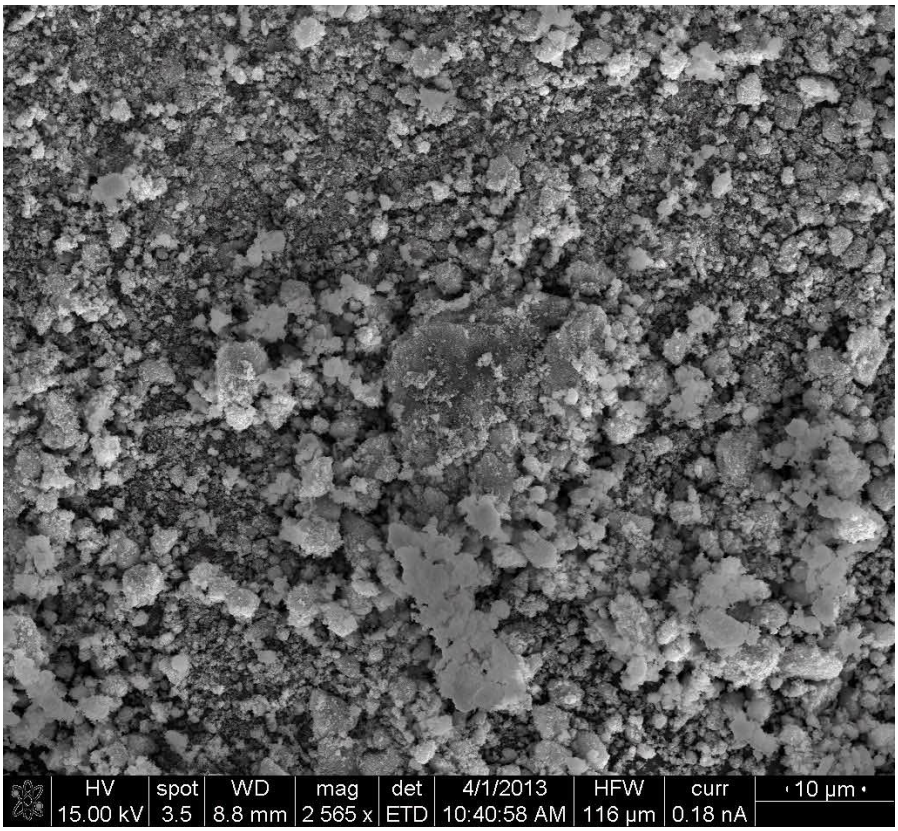

FIGURE 29 – SEM Image for Conventional ZnO

C. Kinetics of Reaction

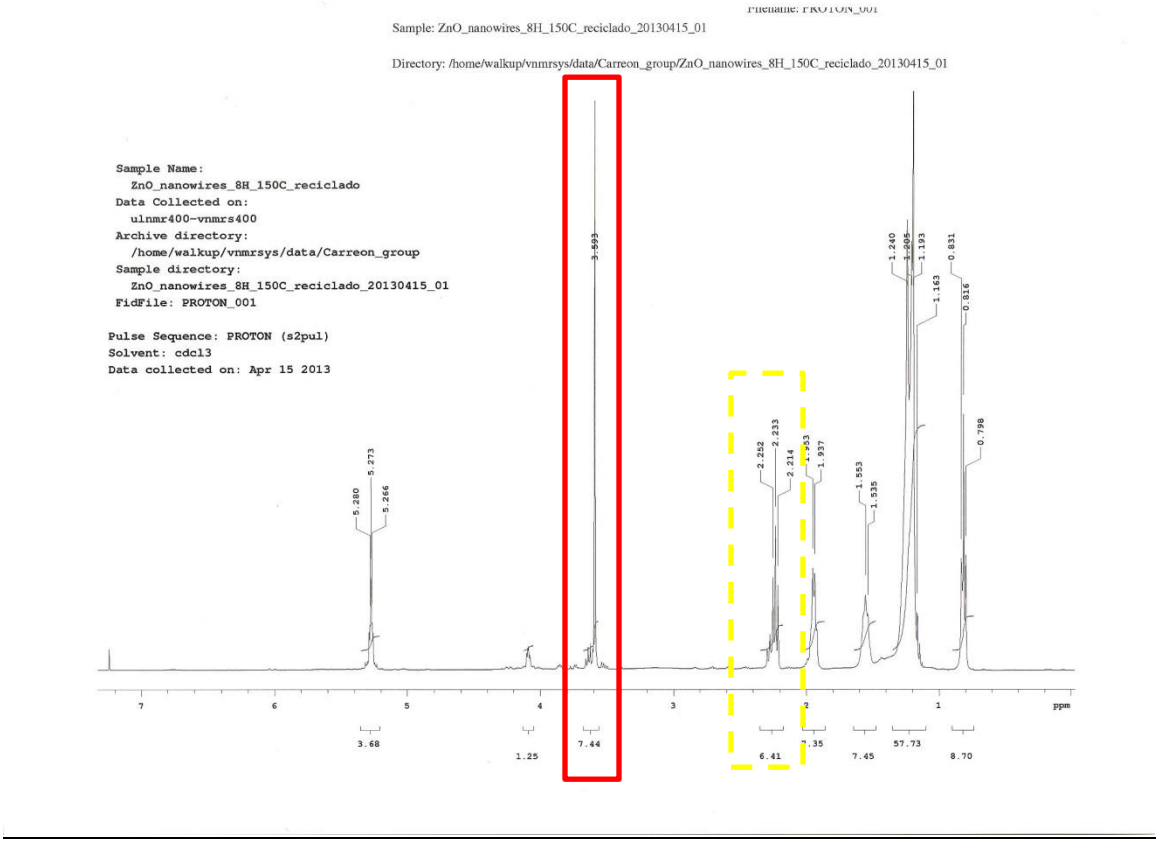

FIGURE 30 – NMR Spectrum for Biodiesel: Methoxy Group (solid box), Methylene Group (dashed box)

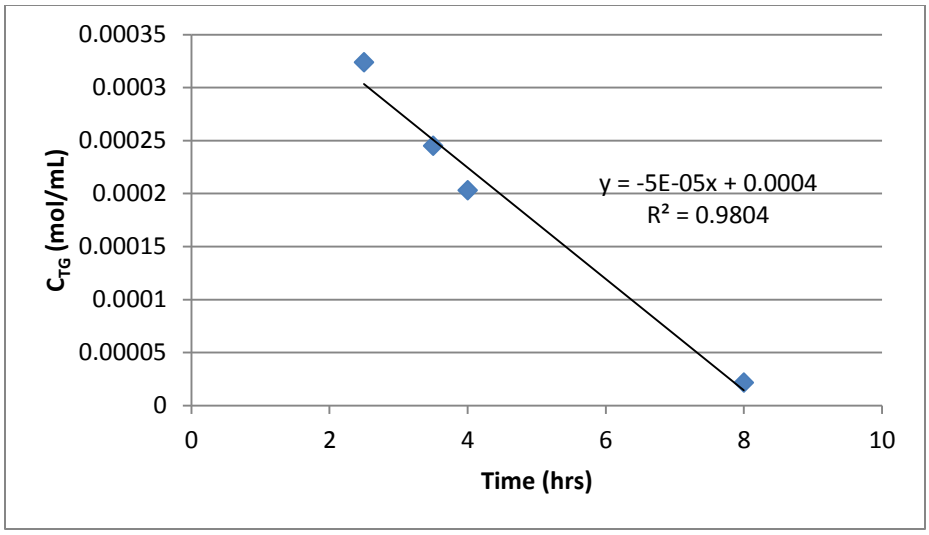

FIGURE 31 – Zero Order Reaction Kinetics for Integral Method

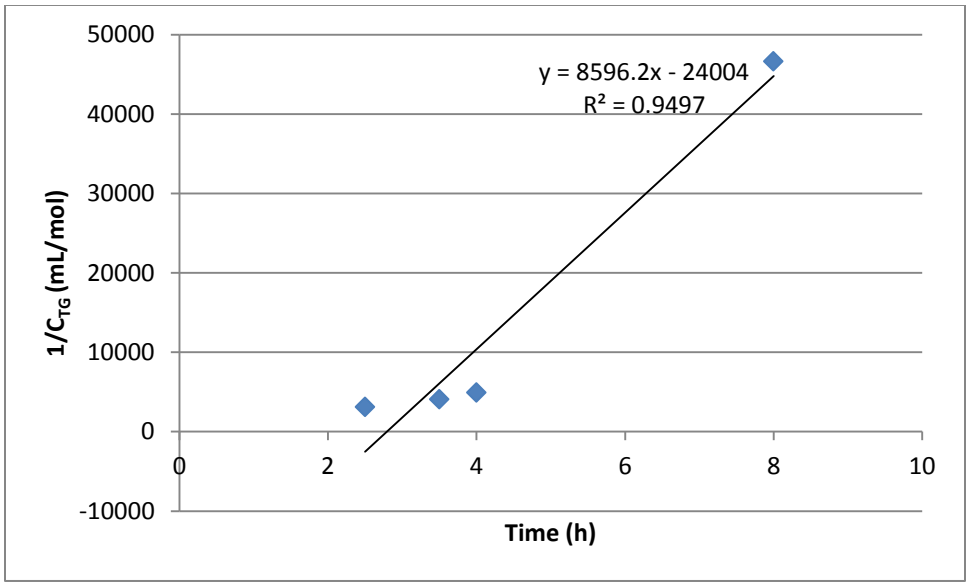

FIGURE 32 – Second Order Integral Method Reaction Kinetics Plot

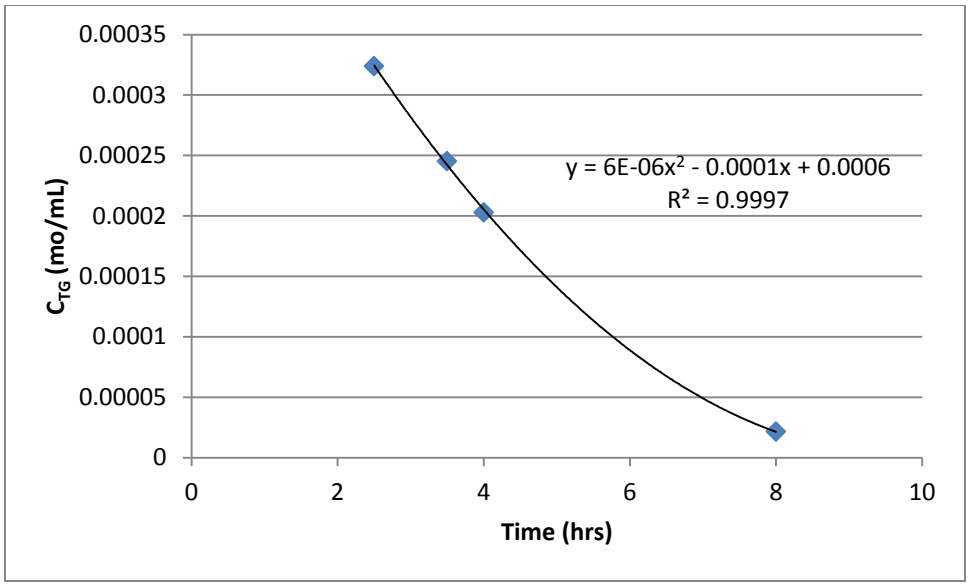

FIGURE 33 – Polynomial Method Fit

VITA

NAME: Carmen Maria Miralda Molina

ADDRESS: 4400 Country View Dr.
Floyds Knobs, IN 47119

DOB: Distrito Central, Honduras – March 10, 1990

EDUCATION & TRAINING:

B.S., Chemical Engineering
University of Louisville
2008-2012

M.Eng., Chemical Engineering
University of Louisville
2012-2013

HONORS & AWARDS:

Departmental Alumni Prize-Chemical Engineering Department, 2013

D. A. Richards/G.E. Memorial Scholarship recipient, J. B. Speed School of Engineering, 2012

Graduate Teaching Assistant, Department of Engineering Fundamentals, J.B. Speed School of Engineering, 2012

Southern Indiana Trustees Scholarship, University of Louisville, 2008-2013

PROFESSIONAL SOCIETIES:

Tau Beta Pi
American Institute of Chemical Engineers
Society of Hispanic Professional Engineers